Research Square

Preprints are preliminary reports that have not undergone peer review.
They should not be considered conclusive, used to inform clinical practice,
or referenced by the media as validated information.

Enhanced antitumor efficacy and safety of cannabidiol-loaded O-carboxymethyl chitosan nanomicelles in hepatocellular carcinoma

Wenhui Ruan
Shanxi Institute of Medicine and Life Science)
Yanlin Kang
Shanxi University of Chinese Medicine
Zhijuan Wu
Shanxi University of Chinese Medicine
Zhihao Chen
Shanxi University of Chinese Medicine
Rui Li
46116288@qq.com
Shanxi University of Chinese Medicine

Research Article

Keywords: Hepatocellular carcinoma, Cannabidiol, O-carboxymethyl chitosan, Nanomicelles, Antitumor efficacy, Biodistribution

Posted Date: April 5th, 2026

DOI: https://doi.org/10.21203/rs.3.rs-9212714/v1

License: This work is licensed under a Creative Commons Attribution 4.0 International License.
Read Full License

Additional Declarations: No competing interests reported.

Version of Record: A version of this preprint was published at BioNanoScience on May 26th, 2026. See the published version at https://doi.org/10.1007/s12668-026-02635-0.

Abstract

Hepatocellular carcinoma (HCC) remains a major global health challenge, and effective drug delivery strategies are still needed to improve therapeutic outcomes. In this study, cannabidiol-loaded O-carboxymethyl chitosan (CBD/CCMC) nanomicelles were evaluated for their biodistribution, antitumor efficacy, and in vivo biosafety in H22 tumor-bearing mice. The results showed that CBD/CCMC nanomicelles exhibited prolonged retention in vivo and enhanced accumulation in tumor tissues, as demonstrated by in vivo fluorescence imaging. Compared with free CBD, the nanomicelle formulation significantly inhibited tumor growth, with a tumor inhibition rate of 53.57% versus 17.04%. In addition, CBD/CCMC nanomicelles effectively maintained body weight and reduced systemic toxicity. Histopathological analysis revealed increased tumor cell apoptosis and necrosis in the treatment group. Furthermore, elevated levels of IL-2 and TNF-α were observed, suggesting a potential modulation of tumor-associated immune responses. Overall, these findings indicate that CCMC-based micelles can enhance tumor accumulation and antitumor activity of CBD while maintaining favorable biosafety, providing a promising delivery strategy for hepatocellular carcinoma treatment.

Introduction

Hepatocellular carcinoma (HCC) is one of the most common types of primary liver cancer worldwide. It accounts for about 90% of all liver cancer cases and is one of the important causes of cancer-related death[1, 2]. As a primary liver malignancy, HCC exhibits profound molecular heterogeneity, which often renders conventional systemic chemotherapies suboptimal due to inadequate tumor infiltration and severe off-target effects [3]. While therapeutic modalities such as surgical resection and targeted molecular therapy (e.g., sorafenib) have progressed, the five-year survival rate remains unsatisfactory [4]. A key pharmacological limitation is that many potent antitumor candidates are hindered by their intrinsic physicochemical properties: notably poor aqueous solubility and rapid systemic clearance [5, 6]. These drawbacks require high therapeutic doses, which inevitably trigger dose-limiting toxicities in clinical practice .

In this context, nano-drug delivery systems (NDDS) have emerged as a pivotal strategy to refine the therapeutic window of lipophilic drugs. By leveraging the enhanced permeability and retention (EPR) effect, nanocarriers can facilitate the passive targeting of tumor tissues, thereby maximizing local drug concentrations while shielding healthy organs from systemic exposure [7, 8]. Among various nanoplatforms, amphiphilic polymer micelles have garnered significant attention due to their unique core-shell architecture, which provides a protective reservoir for hydrophobic payloads[9]. Specifically, natural polysaccharide derivatives like chitosan (CS) are highly valued for their biocompatibility and biodegradability [10, 11]. However, the limited solubility of native CS at physiological pH has prompted the development of derivatives such as O-carboxymethyl chitosan (OCMC). OCMC not only retains the biological merits of CS but also offers enhanced water solubility and functional groups for hydrophobic grafting, making it an ideal candidate for constructing stable, self-assembled nanomicelles [12].

Cannabidiol (CBD), a major non-psychoactive phytocannabinoid derived from Cannabis sativa, has recently been identified as a multi-target anti-tumor agent with promising efficacy against HCC[13, 14]. Unlike traditional cytotoxic drugs, CBD exerts its effects through complex signaling cross-talk. Recent studies have elucidated that CBD can trigger GSDME-mediated pyroptosis in hepatoma cells by inducing mitochondrial stress and an integrated stress response [15]. Furthermore, CBD has been shown to reprogram tumor metabolism by modulating the ATF4-IGFBP1-Akt axis, effectively starving the tumor of essential metabolic intermediates [16]. Despite these compelling bioactivities, CBD's clinical translation is severely bottlenecked by its extreme lipophilicity (log P 6.3) and high first-pass metabolism, leading to an oral bioavailability of less than 6%[17]. Therefore, developing a specialized nano-delivery vehicle is not merely an optimization but a prerequisite for CBD-based HCC therapy.

Our research group previously engineered a novel amphiphilic polymer, O-carboxymethyl chitosan-g-cholesterol succinic acid monoester (CCMC), and demonstrated its capacity to form stable nanomicelles. Our preliminary investigations confirmed that CBD/CCMC nanomicelles significantly enhance the aqueous solubility and pharmacokinetic profile of CBD in healthy animal models[18, 19]. However, a critical knowledge gap remains: the transition from improved pharmacokinetics to tangible therapeutic outcomes in the complex microenvironment of a solid tumor. The actual antitumor efficacy, real-time biodistribution in tumor-bearing hosts, and comprehensive biosafety profile remain to be rigorously evaluated.

In the this study, we aimed to bridge this gap by conducting a multi-dimensional evaluation of CBD/CCMC nanomicelles in H22 HCC-bearing mouse models. We utilized in vivo fluorescence imaging to visualize the spatio-temporal distribution and tumor-retention capabilities of the micelles. The therapeutic potency was quantified through tumor growth kinetics and detailed histopathological analysis of the tumor microenvironment. Crucially, to address the biosafety concerns often overlooked in early-stage nano-formulation studies, we performed an extensive safety assessment, including organ indices, hematological parameters, and systemic biocompatibility assays. The conceptual framework of this study is illustrated in the Graphical Abstract (Fig. 1). By providing a comprehensive preclinical evaluation of this CBD-loaded nanoplatform, this work seeks to validate the shift from material synthesis to effective HCC therapy, offering new insights into the application of cannabinoid-based nanomedicines.

Materials and Methods

Materials

O-carboxymethyl chitosan (OCMC, 50,000 Da, degree of deacetylation 90%, degree of substitution 85%) was purchased from Qingdao Honghai Biotechnology Co., Ltd. (Shandong, China). CBD was obtained from Nanjing Yuanzhi Biotechnology Co., Ltd. Cyclophosphamide (CTX) was purchased from Shanghai Yuanye Biotechnology Co., Ltd. (BR grade, 97%). PBS was obtained from Beijing Solarbio Science & Technology Co., Ltd. 0.9% sodium chloride injection was purchased from Shijiazhuang Siyao Co.,

Ltd. Anhydrous ethanol, Xylene, and Tween 80 were obtained from Tianjin Beichen Fangzheng Reagent Factory. Coumarin 6 was purchased from Shanghai Macklin Biochemical Co., Ltd. (≥98% by HPLC). Universal tissue fixative (neutral) was obtained from Wuhan Servicebio Technology Co., Ltd. Neutral gum was purchased from Sinopharm Chemical Reagent Co., Ltd. Hematoxylin-eosin (HE) staining kit was obtained from Wuhan Servicebio Technology Co., Ltd. ELISA kits for IL-2 and TNF-α were purchased from Shanghai Qifa Experimental Reagent Co., Ltd. Cellmax Chinese fetal bovine serum (premium grade) was obtained from Saiaomei Cell Technology (Beijing) Co., Ltd. McCoy's 5A medium was purchased from Shanghai Bosheng Biotechnology Co., Ltd.

Preparation of CBD/CCMC Nanomicelles

The preparation method of CBD/CCMC nanomicelles was performed as described in previous literature[18,19]. Briefly, cholesterol (CHOL) and succinic anhydride were reacted to form an ester under the catalysis of 4-dimethylaminopyridine. The exposed single carboxyl group reacted with the amino group on the side chain of OCMC under the synergistic catalysis of EDC·HCl and NHS to form an amide, that is, the amphiphilic polymer CCMC.

20 mg of CCMC was dissolved in 2 mL of deionized (DI) water, stirred at 25 ℃ for 12 h, and sonicated in an ice bath. After filtration through a 0.22 μm microporous filter membrane, the resulting filtrate was lyophilized to obtain CCMC nanomicelles. 20 mg of CCMC nanomicelles was dissolved in 5 mL of DI water. 2 mg of CBD was dissolved in an appropriate amount of tetrahydrofuran and added dropwise to the CCMC nanomicelles aqueous solution. The mixture was dialyzed against DI water for 24 h. After filtration of the dialysate through a 0.45 μm filter membrane, CBD/CCMC nanomicelles were obtained by lyophilization.

Characterization of CBD/CCMC Nanomicelles

Particle Size and Zeta Potential

The CBD/CCMC nanomicelles solution was placed in a sample pool. The particle size, zeta potential, and PDI of CBD/CCMC nanomicelles (1 mg/mL) were determined using a Zetasizer Nano ZS90 laser particle size analyzer (Malvern PANalytical Ltd., UK). All measurements were performed at 25 ℃, with three parallel determinations, and the average value was calculated.

Drug Loading and Encapsulation Efficiency

5 mg of CBD/CCMC nanomicelles was dissolved in 1 mL of DI water, and 9 mL of acetonitrile was added. The mixture was sonicated for depolymerization (350 W, 30 min) and filtered through a 0.22 μm microporous filter membrane. The CBD content was detected using a Waters e2695 HPLC system (Waters Corporation, USA). The EE% and DLC% were calculated according to the following formulas:

$$EE/\%=m/m_0 \times 100\%$$

$$DLC/\%=m/m_1 \times 100\%$$

Where m is the weight of the drug in the nanomicelles; m_0 is the weight of the drug; and m_1 is the weight of the drug-loaded micelles.

Establishment of the H22 Tumor-Bearing Mouse Model

The H22 cell line was purchased from Shanghai Zhongqiao XINZHOU Biotechnology Co., Ltd. SPF male KM mice (25 ± 2 g) were obtained from SPF (Beijing) Biotechnology Co., Ltd. This experiment was approved by the Animal Ethics Committee of Shanxi University of Chinese Medicine (Ethics Approval No.: AWE202403289).

After resuscitation, H22 cells were cultured to the logarithmic growth phase, collected, and washed three times with PBS to remove serum. The cell concentration was adjusted to 3×10^7 cells/mL, and 0.8 mL was intraperitoneally injected into mice. Ascites was collected after 9 d, diluted with PBS, and passaged to the third generation using the same method. Ascites from the third-generation tumor-bearing mice was collected, washed 3 times with PBS, counted, and the cell concentration was adjusted to 2.5×10^7 cells/mL. A 0.2 mL aliquot was subcutaneously inoculated into the axilla of the right forelimb of male KM mice. The model was considered successfully established when the tumor volume reached 100-150 mm^3.

Tumor-bearing mice were randomly divided into 5 groups (n=10): Normal control group (NC group), model group, CTX group (20 mg/kg), CBD group, and CBD/CCMC nanomicelles group. Drugs were administered by intraperitoneal injection once every 2 d for 14 consecutive days. The dosage of CBD in both the CBD group and CBD/CCMC nanomicelles group was 20 mg/kg (calculated by CBD).

***In Vivo* Biodistribution**

CCMC nanomicelles were labeled with the fluorescent probe C6 to evaluate their *in vivo* biodistribution in H22 tumor-bearing mice. 12 of H22 tumor-bearing mice were randomly divided into 2 groups (6 mice per group), and free C6 and C6/CCMC nanomicelles were intraperitoneally injected respectively (C6 dosage: 0.8 μg/kg). At 1, 6, 12, and 24 h after administration, whole-body fluorescent signals of mice were collected using a small animal in vivo imaging system (AniView SE, Guangzhou Boluteng Biotechnology Co., Ltd.). Mice were sacrificed 24 h after administration, and heart, liver, spleen, lung, kidney, and tumor tissues were dissected and separated. After washing with PBS, the tissues were placed under the imaging system for fluorescence imaging.

***In Vivo* Anti-tumor Efficacy Evaluation**

The body weight of mice was measured before each administration, and their mental state and survival status were recorded. After the last administration, mice were euthanized by intravenous injection of a barbiturate-containing euthanasia solution. Tumor, thymus, spleen, liver, and kidney tissues were

dissected and separated. The net body weight, tumor volume, organ indies, and tumor inhibition rate were calculated according to the following formulas:

$$Net\ body\ weight = mouse\ body\ weight - tumor\ mass$$

$$tumor\ volume\ V\ (mm^3) = D\ (mm) \times d\ (mm)^2/2$$

$$Tumor\ inhibit\ rate(\%) = (W_{control} - W_{test})\ /W_{control} \times 100\%$$

$$Organ\ index = Organ\ weight\ /Mice\ weight \times 100\%$$

$W_{control}$ is the tumor weight of the model group and W_{test} is the tumor weight of the treatment group. D and d represent the maximum diameter (D) and minimum diameter (d) of the tumor measured with a vernier caliper.

Histopathological Analysis

After the end of administration, tumor tissues of mice in each group were stripped and fixed in 4% paraformaldehyde solution for 48 h. After gradient ethanol dehydration, xylene clearing, paraffin infiltration, and embedding, continuous sections with a thickness of 4 μm were prepared. The sections were deparaffinized with xylene, hydrated with gradient ethanol, stained with HE, then dehydrated with gradient ethanol, cleared with xylene, and mounted with neutral gum. The pathological characteristics of tumor tissues in each group were observed using an Axiolab5 optical microscope (Carl Zeiss (Shanghai) Management Co., Ltd., China), and analyzed using ImageJ software.

Hematological Analysis

After the end of administration, mice in each group were fasted for 12 h with free access to water. Before euthanasia, 0.5 mL of blood was collected into EDTA-K2 anticoagulant tubes. Hematological analysis was performed using a Hemavet 950FS automatic hematology analyzer (Beijing Zhuoyuelixin Scientific Instrument Co., Ltd., China) to evaluate the effect of CBD/CCMC nanomicelles on the hematological system of H22 tumor-bearing mice.

Cytokine Analysis by ELISA

After the end of administration, 1 mL of blood sample was collected. After overnight storage at 4 ℃, serum was separated by centrifugation at 3000 rpm for 15 min. The levels of TNF-α, and IL-2 in serum were detected according to the instructions of the ELISA kits.

Statistical analysis

All experiments were performed at least in triplicate. Data were expressed as mean ± standard deviation (SD). Statistical analysis was conducted using GraphPad Prism software. Differences between groups

were analyzed using one-way analysis of variance (ANOVA). A value of $P < 0.05$ was considered statistically significant.

Results and Discussion

Characterization of CBD/CCMC Nanomicelles

Dynamic light scattering (DLS) was used to characterize the particle size, PDI, and zeta potential of CBD/CCMC nanomicelles. The results showed that the average particle size of CBD/CCMC nanomicelles was 205.33 ± 2.17 nm, the PDI was 0.11 ± 0.06, and the zeta potential was − 19.25 ± 1.56 mV. The low PDI value indicated that the nanomicelles had a relatively uniform particle size distribution[20]. The surface was negatively charged, which helped maintain the colloidal stability of the micelles in aqueous solution and reduce non-specific adsorption with plasma proteins to a certain extent, thereby improving the circulatory stability in vivo[21].

In addition, the EE% and DLC% of CBD/CCMC nanomicelles were 83.49% ± 0.63% and 8.96% ± 0.29%, respectively. The high EE% indicated that the nanomicelle system could effectively encapsulate the hydrophobic drug CBD. This may be related to the hydrophobic core structure formed by the CCMC polymer, which is conducive to improving the EE% of CBD in the micelles[22].

In Vivo Biodistribution of CBD/CCMC Nanomicelles

To evaluate the *in vivo* distribution characteristics of CBD/CCMC nanomicelles, C6 was used as a fluorescent probe to label the nanomicelles, and an AniView SE small animal in vivo imaging system was used to observe the in vivo fluorescence imaging of H22 tumor-bearing mice. As shown in Fig. 2A, fluorescent signals could be detected in the abdominal cavity of mice 1 h after intraperitoneal injection of free C6 and C6/CCMC nanomicelles. With the extension of time, the fluorescent signals in the two groups of mice gradually increased and spread to surrounding tissues. Among them, the fluorescent signal of the C6/CCMC nanomicelles group was overall stronger than that of the free C6 group, and reached a high level at 6–12 h. This suggested that the nanomicelles system could maintain a long circulation time *in vivo*, which was beneficial to the distribution and accumulation of drugs in tissues. No obvious fluorescent signal was observed at the tumor site in either group of mice. This may be because the tumor tissue was located deep under the skin, and the fluorescent signal was blocked by the skin and surrounding tissues, making it difficult to detect directly through the in vivo imaging system[23, 24].

To further clarify the tissue distribution of C6 in vivo, mice were sacrificed 24 h after administration, and major organs (heart, liver, spleen, lung, kidney) and tumor tissues were separated for ex vivo fluorescence imaging. As shown in Fig. 2B, the fluorescent signal in the tumor tissue of the free C6 group was weak, while the C6/CCMC nanomicelles group showed a more obvious fluorescent signal in the tumor tissue. This suggested that the nanomicelles carrier helped promote the accumulation of C6 at the tumor site. This phenomenon may be related to the EPR effect of nanomicelles in tumor tissues[25]. Due to the abnormal vascular structure, increased permeability, and defective lymphatic

reflux function of tumors, nanomicelles are more likely to enter tumor tissues and remain there, thereby achieving passive targeted accumulation[26, 27]. In addition, strong fluorescent signals were detected in the livers of both groups of mice, which was more obvious in the C6/CCMC nanomicelles group. This may be because after entering the blood circulation, nanomicelles are easily phagocytized and cleared by Kupffer cells in the liver reticuloendothelial system, leading to their accumulation in the liver[28]. Therefore, compared with free C6, C6/CCMC nanomicelles can improve the enrichment level of fluorescent probes in tumor tissues, indicating that the nano-delivery system has potential tumor-targeted delivery ability.

In Vivo Antitumor Efficacy

Body Weight and Systemic Condition

The changes in body weight and overall condition of mice in each group are shown in Fig. 2C. Mice in the NC group showed stable weight gain over time and good mental state. Mice in the model group also showed a continuous upward trend in body weight, but tumor burden-related manifestations such as decreased mental state and reduced hair luster were observed during the experiment. Mice in the CTX group showed a significant decrease in body weight at the initial stage of administration, followed by a slight recovery, but the final body weight was still the lowest among all groups, accompanied by decreased activity and appetite. This may be related to the systemic toxicity caused by CTX. The studies have shown that cytotoxic chemotherapeutic drugs can cause weight loss by inducing myelosuppression and gastrointestinal toxicity[29]. In contrast, mice in the CBD group showed a slow weight gain trend, but their overall condition was still poor. Notably, the body weight of mice in the CBD/CCMC nanomicelles group changed relatively stably and showed a continuous slow growth trend. The mice had normal diet and drinking water and good mental state, indicating that the nanomicelles had good in vivo tolerance. The studies have shown that polymer nanomicelles can improve the stability of drugs *in vivo* and reduce adverse effects on normal tissues through their core-shell structure, thereby reducing systemic toxicity to a certain extent[30].

Since the tumor weight of tumor-bearing mice accounts for a large proportion of the body weight, it may interfere with the evaluation of body weight. Therefore, the net body weight of mice was further calculated according to the formula to more accurately reflect the effect of drugs on the overall state of the body (Fig. 2D). The results showed that compared with the NC group, the net body weight of mice in the model group, CTX group, and CBD group was significantly reduced, while there was no significant difference between the CBD/CCMC nanomicelles group and the NC group. In addition, compared with the CBD group, the net body weight of mice in the CBD/CCMC nanomicelles group was significantly increased. This result suggests that the nanomicelles can reduce body consumption caused by tumor burden. Meanwhile, they exert an antitumor effect and help maintain metabolic homeostasis and body weight stability in mice.

Tumor Weight and Tumor Inhibition Rate

The tumor weight and tumor inhibition rate of mice in each group are shown in Fig. 2E-F, and the solid tumors of mice in each group are shown in Fig. 2G. Mice in the model group had large tumor volume and significantly increased tumor weight, indicating that the H22 tumor-bearing mouse model was successfully established. Compared with the model group, the tumor weight of mice in each administration treatment group was significantly reduced, indicating that different treatment schemes had a certain inhibitory effect on tumor growth. Further comparison of the anti-tumor effects of different treatment groups found that the CTX group had the lowest tumor weight, showing the strongest anti-tumor activity with a tumor inhibition rate of 65.02%. The tumor inhibition rate of the CBD group was 17.04%, suggesting that free CBD had a certain inhibitory effect on H22 tumors, but the effect was limited. In contrast, the tumor inhibition rate of the CBD/CCMC nanomicelles group reached 53.57%, which was significantly higher than that of the CBD group, indicating that the nanomicelles delivery system could significantly enhance the antitumor effect of CBD. This enhancement may be related to the improvement of solubility and *in vivo* stability of hydrophobic drugs by nanomicelles. Studies have shown that polymer nanomicelles can encapsulate poorly soluble drugs via their hydrophobic core[31, 32]. This strategy significantly improves the water solubility, stability, and bioavailability of drugs, thus enhancing their in vivo anti-tumor activity[33]. In addition, nanoscale carriers can passively accumulate at tumor sites through the EPR effect of tumor tissues. This further increases the local drug concentration in tumor tissues[34]. Therefore, CBD/CCMC nanomicelles exhibit better anti-tumor activity than free CBD.

Organ Index

The thymus is the main organ for T lymphocyte differentiation and maturation, while the spleen is rich in T/B lymphocytes and macrophages, which is an important supporting organ for the body's immune response[35]. Therefore, the thymus index and spleen index can reflect the effect of drugs on immune function to a certain extent. As shown in Fig. 3A-D, compared with the NC group, the thymus index of the model group was significantly decreased, and the spleen index was increased, suggesting that tumor burden may lead to immunosuppression and compensatory extramedullary hematopoiesis[36]. Compared with the Model group, both the thymus and spleen indexes of the CTX treatment group were significantly decreased, which was consistent with the known immunosuppressive effect of CTX and the mechanism of immune organ atrophy[37]. In contrast, the thymus index of the CBD/CCMC nanomicelles group was significantly higher than that of the CTX group. Meanwhile, the spleen index was slightly lower than that of the CBD group. These results indicate that CBD delivered by nanomicelles can protect immune organs to a certain extent. It also reduces the damage induced by tumors and chemotherapeutic drugs. This effect may be related to the immunomodulatory activity of CBD, such as promoting T cell survival and inhibiting the secretion of inflammatory factors[38, 39].

In addition, compared with the NC group, the liver and kidney indexes of the CTX group and free CBD group were significantly increased in terms of liver and kidney indexes. Anatomical observation showed hepatomegaly and pale surface, suggesting potential hepatotoxicity and nephrotoxicity. In contrast, the liver index of the CBD/CCMC nanomicelles group was close to that of the NC group, and the kidney index

was significantly lower than that of the CTX and CBD groups. This indicated that the nanomicelles could reduce toxicity to the liver and kidney while ensuring drug delivery efficiency. This is consistent with reports that polymer nanomicelles improve the in vivo distribution of drugs and reduce exposure to non-target organs[33]. It suggests that CBD/CCMC nanomicelles show good biocompatibility and safety to immune organs and major organs while efficiently delivering drugs, providing experimental basis for their further clinical application.

Histopathological Analysis

The HE staining results of tumor tissues from H22 liver cancer model mice are shown in Fig. 3E. In the model group, tumor cells were distributed in dense nests with hypertrophic and distinct nucleoli. The nuclear-cytoplasmic ratio was increased, and the nuclei were stained dark purple-blue. These features indicated that tumor cells were in a highly proliferative state with obvious malignant characteristics. In the CTX group, the number of tumor cell nuclei was significantly decreased, and the cells were loosely and irregularly arranged.These changes demonstrated typical proliferation inhibition and cell killing effects mediated by chemotherapeutic drugs[40]. Both the CBD monomer group and the CBD/CCMC nanomicelles group exhibited lighter nuclear staining, fewer nuclei, and smaller cell volumes.The tissue gaps were widened, and the necrotic foci were significantly larger than those in the model group. Notably, the histological changes in the CBD/CCMC nanomicelles group were similar to those in the CTX group. The features of tumor cell necrosis and apoptosis were more obvious in this group. These results suggested that CBD/CCMC nanomicelles can improve the targeted accumulation of CBD in tumor tissues via nanocarriers.Thus, they can effectively inhibit the proliferation and induce the apoptosis of hepatocellular carcinoma cells.

Hematological Analysis

After 14 d of administration, the results of blood routine detection of mice in each group are shown in Fig. 4A-G. Compared with the model group, the white blood cells (WBC), lymphocytes (LYM) and platelets (PLT) of mice in the CTX group were significantly decreased. Monocytes (MON), neutrophils (NEU), and red blood cells (RBC) showed a downward trend, but the difference was not statistically significant. This phenomenon was associated with the non-selective inhibition of rapidly proliferating tissues (such as bone marrow and lymphoid tissues) by phosphoramide mustard, the active metabolite of CTX.Such inhibition led to impaired immunity and suppressed hematopoietic function in mice[41]. Compared with the CTX group, the levels of WBC, LYM, MON, and PLT in the CBD group were partially restored. In contrast, the levels of WBC, LYM, RBC, and PLT in the CBD/CCMC nanomicelles group were significantly elevated. In particular, the recovery of RBC and PLT was more pronounced. Further analysis demonstrated that compared with the NC group, several hematological parameters in the CBD group still showed significant differences. However, all indicators in the CBD/CCMC nanomicelles group were close to normal levels. These results indicated that CBD/CCMC nanomicelles could maintain hematological homeostasis. Therefore, CBD/CCMC nanomicelles exhibited favorable biocompatibility and biosafety.

Cytokine Analysis

IL-2 and TNF-α are key factors regulating T cell proliferation, immune homeostasis, and anti-tumor immune response[42]. In this experiment, As shown in the Fig. 4H-I, the CTX group was independently grouped as a positive anti-tumor drug, which could effectively inhibit tumor growth, but the serum levels of IL-2 and TNF-α were significantly decreased. This reflected that CTX had immunosuppressive side effects while exerting anti-tumor effect. Compared with model group, the CBD group showed limited improvement in the levels of immune factors. And the levels of IL-2 and TNF-α in the CBD/CCMC nanomicelles group were significantly increased. These elevated immune factor levels were close to those in the NC group. Moreover, the improvement in the CBD/CCMC nanomicelles group was significantly better than that in the CBD group. These results indicated that CBD/CCMC nanomicelles could effectively inhibit tumor growth. Additionally, they could reverse tumor-induced immunosuppression to a certain extent. This effect was achieved by enhancing the targeted delivery of CBD at the tumor site, thereby boosting the body's antitumor immune response.

Conclusion

This study demonstrated that CBD/CCMC nanomicelles exerted significant antitumor activity and favorable in vivo biosafety in H22 tumor-bearing mice. In vivo fluorescence imaging revealed that the nanomicelles prolonged blood circulation time and effectively accumulated in tumor tissues, indicating typical passive tumor-targeting ability mainly attributed to the EPR effect. Compared with free CBD, CBD/CCMC nanomicelles significantly suppressed tumor growth, and histological analysis confirmed enhanced tumor cell apoptosis and necrosis. Meanwhile, CBD/CCMC nanomicelles alleviated the reduction in body weight, ameliorated abnormal routine blood parameters, and reduced pathological damage to major immune organs, liver, and kidney, suggesting that the nanomicelle formulation effectively reduced the systemic toxicity of CBD. Furthermore, serum immune factor analysis showed that CBD/CCMC nanomicelles elevated the levels of IL-2 and TNF-α, implying that they could partially reverse tumor-induced immunosuppression and enhance the antitumor immune response. In summary, this work validates that CBD/CCMC nanomicelles improve tumor-targeted delivery, enhance antitumor efficacy, and improve the biosafety of CBD, providing a promising experimental basis for further clinical translation of CBD in the treatment of hepatocellular carcinoma.

Declarations

Funding

This work was supported financially by the Basic Research Project of Shanxi Province (201801D221278) and the Horizontal project (2022-05).

Animal Ethics

Animal Ethics All animal experiments were performed in accordance with the Guidelines for the Care and Use of Laboratory Animals of China. The experimental protocols were reviewed and approved by the

Animal Ethics Committee of Shanxi University of Chinese Medicine (Ethics approval number: AWE202403289).

Author contribution

Wenhui Ruan: Data curation, Writing - original draft. Yanlin Kang: Methodology, Investigation. Zhijuan Wu: Supervision, Visualization. Zhihao Chen: Methodology, Formal analysis. Rui Li: Conceptualization, Writing original draft, Writing review & editing, Supervision.

Data availability

Data will be made available on request.

Conflict of interest

The authors declare that they have no competing financial interests or personal relationships that may have influenced the work reported in this study.

References

1. Llovet, J. M., Kelley, R. K., Villanueva, A., et al. (2021). Hepatocellular carcinoma. *Nat Rev Dis Primers*, *7*(1), 6. https://doi.org/10.1038/s41572-020-00240-3
2. Tianzuo Zhan, J., Betge, N., Schulte, et al. (2025). Digestive cancers: mechanisms, therapeutics and management. *Signal Transduct Tar*, *10*(1), 24. https://doi.org/10.1038/s41392-024-02097-4
3. Sung, H., Ferlay, J., Siegel, R. L., Laversanne, M., Soerjomataram, I., Jemal, A., & Bray, F. (2021). Global Cancer Statistics 2020: GLOBOCAN Estimates of Incidence and Mortality Worldwide for 36 Cancers in 185 Countries. *CA-Cancer J Clin*, *71*(3), 209–249. https://doi.org/10.3322/caac.2166
4. Zou, Y., Wan, X., Zhou, Q., Zhu, G., Lin, S., Tang, Q., Yang, X., & Wang, X. (2025). Mechanisms of drug resistance in hepatocellular carcinoma. *Biol Proced Online*, *27*(1), 19. https://doi.org/10.1186/s12575-025-00281-6
5. Vargason, A. M., Anselmo, A. C., & Mitragotri, S. (2021). The evolution of commercial drug delivery technologies. *Nat Biomed Eng*, *5*(9), 951–967. https://doi.org/10.1038/s41551-021-00698-w
6. Neil Desai. (2012). Challenges in Development of Nanoparticle-Based Therapeutics. *The AAPS Journal*, *14*(2), 282–295. https://doi.org/10.1208/s12248-012-9339-4
7. Latifa, W., Allahou, S. Y., Madani, Alexander, M., & Seifalian (2021). Investigating the Application of Liposomes as Drug Delivery Systems for the Diagnosis and Treatment of Cancer. *Int J Biomater*, 1–16. https://doi.org/10.1155/2021/3041969
8. Wilhelm, S., Tavares, A. J., Dai, Q., Ohta, S., Audet, J., Dvorak, H. F., & Chan, W. C. (2016). Analysis of nanoparticle delivery to tumours. *Nat Rev Mater*, *1*(5), 16014. https://doi.org/10.1038/natrevmats.2016.14

9. Kuperkar, K., Patel, D., Atanase, L. I., & Bahadur, P. (2022). Amphiphilic block copolymers: their structures, and self-assembly to polymeric micelles and polymersomes as drug delivery vehicles. *Polymers*, *14*(21), 4702. https://doi.org/10.3390/polym14214702
10. Saravanakumar, G., Kim, J., & Kim, W. J. (2021). Recent advances in functional nanocarriers based on natural polysaccharides for cancer therapy. *Carbohyd Polym*, *221*, 94–106. https://doi.org/10.1016/j.reactfunctpolym.2021.104970
11. Jayachandran Venkatesan, S. K. Kim (2010). Chitosan Composites for Bone Tissue Engineering—An Overview. *Marine Drugs*, *8*(8), 2252–2266. https://doi.org/10.3390/md8082252
12. Yadav, N., Mudgal, D., Anand, R., Jindal, S., & Mishra, V. (2022). Recent development in nanoencapsulation and delivery of natural bioactives through chitosan scaffolds for various biological applications. *International Journal Of Biological Macromolecules*, *220*, 537–572. https://doi.org/10.1016/j.ijbiomac.2022.08.098
13. Linciano, P., Citti, C., Russo, F., Tolomeo, F., Laganà, A., Capriotti, A. L., & Cannazza, G. (2020). Identification of a new cannabidiol n-hexyl homolog in a medicinal cannabis variety with an antinociceptive activity in mice: cannabidihexol. *Sci Rep-UK*, *10*(1), 22019. https://doi.org/10.1038/s41598-020-79042-2
14. Esmaeli, M., & Dehghanpour Dehabadi, M. (2025). Cannabidiol (CBD) as a potential therapeutic agent for liver cancer: a comprehensive review of current evidence. *Cancer Cell International*, *25*(1), 215. https://doi.org/10.1186/s12935-025-03870-3
15. Shangguan, F., Zhou, H., Ma, N., Wu, S., Huang, H., Jin, G., & Lan, L. (2021). A Novel Mechanism of Cannabidiol in Suppressing Hepatocellular Carcinoma by Inducing GSDME Dependent Pyroptosis. *Front Cell Dev Biol*, *9*, 697832. https://doi.org/10.3389/fcell.2021.697832
16. Jeon, Y., Kim, T., Kwon, H., Kim, J. K., Park, Y. T., Ham, J., & Kim, Y. J. (2023). Cannabidiol Enhances Cabozantinib-Induced Apoptotic Cell Death via Phosphorylation of p53 Regulated by ER Stress in Hepatocellular Carcinoma. *Cancers*, *15*(15), 3987. https://doi.org/10.3390/cancers15153987
17. Sedlmayr, V., Horn, C., Wurm, D. J., Spadiut, O., & Quehenberger, J. (2023). Archaeosomes facilitate storage and oral delivery of cannabidiol. *Int J Pharmaceut*, *645*, 123434. https://doi.org/10.1016/j.ijpharm.2023.123434
18. Li, R., Ruan, W., Hao, R., Chen, J., Xu, C., Lu, L., & Wang, Y. (2025). O-carboxymethyl chitosan-grafted-cholesterol succinic acid monoester nanomicelles improve oral absorption of cannabidiol: Preparation, intestinal absorption in vitro, and pharmacokinetics in vivo. *J Drug Deliv Sci Tec*, *107*, 106763. https://doi.org/10.1016/j.jddst.2025.106763
19. Li, R., Hao, R., Xu, C., Chen, J., Lu, L., Wang, Y., & Ruan, W. (2024). Preparation, optimisation, and properties of O-carboxymethyl chitosan-g-cholesterol succinic acid monoester polymer nanomicelles. *Biomed Mater (Bristol England)*, *19*(5), 055036. https://doi.org/10.1088/1748-605X/ad6dc5
20. Masarudin, M. J., Cutts, S. M., Evison, B. J., Phillips, D. R., & Pigram, P. J. (2015). Factors determining the stability, size distribution, and cellular accumulation of small, monodisperse chitosan

nanoparticles as candidate vectors for anticancer drug delivery: application to the passive encapsulation of [14C]-doxorubicin. *Nanotechnol Sci Appl*, *8*, 67. https://doi.org/10.2147/NSA.S91785

21. Mashal, M., Attia, N., Grijalvo, S., Eritja, R., Puras, G., & Pedraz, J. L. (2023). Stability of polymeric cationic niosomes and their plasmid DNA-based complexes as gene delivery carriers. *Drug Deliv*, *30*(1). https://doi.org/10.1080/10717544.2023.2219420
22. Li, R., Wu, Z., Lu, L., Kang, Y., Chen, J., Wang, Y., & Ruan, W. (2025). O-carboxymethyl chitosan-g-cholesterol derivative nanomicelles functionalized with folic acid for targeted cannabidiol delivery to ovarian cancer cells. *Journal Of Nanoparticle Research*, *27*, 293. https://doi.org/10.1007/s11051-025-06489-7
23. Kulkarni, M. B., Reed, M. S., Cao, X., García, H. A., Ochoa, M., Jiang, S., & Pogue, B. W. (2025). Combined dual-channel fluorescence depth sensing of indocyanine green and protoporphyrin IX kinetics in subcutaneous murine tumors. *Journal Of Biomedial Optics*, *30*(S1), S13709–S13709. https://doi.org/10.1117/1.JBO.30.S1.S13709
24. Isuri, R. K., Williams, J., Rioux, D., Dorval, P., Chung, W., Dancer, P. A., & Delikatny, E. J. (2025). Clinical Integration of NIR-II Fluorescence Imaging for Cancer Surgery: A Translational Evaluation of Preclinical and Intraoperative Systems. *Cancers*, *17*(16), 2676. https://doi.org/10.3390/cancers17162676
25. Bharate, G. Y., Qin, H., & Fang, J. (2022). Poly(Styrene-Co-Maleic Acid)-Conjugated 6-Aminofluorescein and Rhodamine Micelle as Macromolecular Fluorescent Probes for Micro-Tumors Detection and Imaging. *J Pers Med*, *12*(10), 1650. https://doi.org/10.3390/jpm12101650
26. Nguyen, L. N., Ngo, W., Lin, Z. P., Sindhwani, S., MacMillan, P., Mladjenovic, S. M., & Chan, W. C. (2024). The mechanisms of nanoparticle delivery to solid tumours. *Nat Rev Bioeng*, *2*, 201–213. https://doi.org/10.1038/s44222-024-00154-9
27. Kim, J., Cho, H., Lim, D. K., Joo, M. K., & Kim, K. (2023). Perspectives for Improving the Tumor Targeting of Nanomedicine via the EPR Effect in Clinical Tumors. *International Journal Of Molecular Sciences*, *24*(12), 10082. https://doi.org/10.3390/ijms241210082
28. He, Y., Wang, Y., Wang, L., Jiang, W., & Wilhelm, S. (2024). Understanding nanoparticle-liver interactions in nanomedicine. *Expert Opin Drug Del*, *21*(6), 829–843. https://doi.org/10.1080/17425247.2024.2375400
29. Zhang, Z., Pan, T., Liu, C., Shan, X., Xu, Z., Hong, H., & Sun, H. (2021). Cyclophosphamide induced physiological and biochemical changes in mice with an emphasis on sensitivity analysis. *Ecotox Environ Safe*, *211*, 111889. https://doi.org/10.1016/j.ecoenv.2020.111889
30. Porjazoska Kujundziski, A., & Chamovska, D. (2025). Polymeric Nanomicelles for Cancer Nanomedicine. Engineering Proceedings 99(1):12. https://doi.org/10.3390/engproc2025099012
31. Emadi, R., Amiri, Z., Moghadam, F. M., Raoufi, S., Moradi, M. Z., Asadi, S., & Huh, Y. S. (2026). Self-assembling nanocomposites for smart drug delivery: towards personalized and stimuli-responsive therapeutics. *Rsc Adv*, *16*(6), 5088–5127. https://doi.org/10.1039/d5ra07117h

32. Terreni, E., Zucchetti, E., Tampucci, S., Burgalassi, S., Monti, D., & Chetoni, P. (2021). Combination of Nanomicellar Technology and In Situ Gelling Polymer as Ocular Drug Delivery System (ODDS) for Cyclosporine-A. *Pharmaceutics*, *13*(2), 192. https://doi.org/10.3390/pharmaceutics13020192
33. Hwang, D., Ramsey, J. D., & Kabanov, A. V. (2020). Polymeric micelles for the delivery of poorly soluble drugs: From nanoformulation to clinical approval. *Adv Drug Deliver Rev*, *156*, 80–118. https://doi.org/10.1016/j.addr.2020.09.009
34. Maeda, H., Wu, J., Sawa, T., Matsumura, Y., & Hori, K. (2000). Tumor vascular permeability and the EPR effect in macromolecular therapeutics: a review. *Journal Of Controlled Release : Official Journal Of The Controlled Release Society*, *65*(1–2), 271–284. https://doi.org/10.1016/S0168-3659(99)00248-5
35. Hirakawa, R., Nurjanah, S., Furukawa, K., Murai, A., Kikusato, M., Nochi, T., & Toyomizu, M. (2020). Heat Stress Causes Immune Abnormalities via Massive Damage to Effect Proliferation and Differentiation of Lymphocytes in Broiler Chickens. *Front Vet Sci*, *7*, 46. https://doi.org/10.3389/fvets.2020.00046
36. Chen, Z., Cheng, X., Yang, L., Cheng, X., Zhu, B., & Long, H. (2023). Mechanism and effects of extramedullary hematopoiesis on anti-tumor immunity. *Cancer Biol Med*, *20*(7), 477. https://doi.org/10.20892/j.issn.2095-3941.2023.0203
37. Zhou, Q., Gao, J., Sun, X., Du, J., Wu, Z., Liang, D., & Fang, B. (2024). Immunomodulatory mechanisms of tea leaf polysaccharide in mice with cyclophosphamide-induced immunosuppression based on gut flora and metabolomics. *Foods*, *13*(18), 2994. https://doi.org/10.3390/foods13182994
38. Liu, J., Pan, D., Huang, X., Wang, S., Chen, H., Zhu, Y. Z., & Ye, L. (2023). Targeting collagen in tumor extracellular matrix as a novel targeted strategy in cancer immunotherapy. *Frontiers In Oncology*, *13*, 1225483. https://doi.org/10.3389/fonc.2023.1225483
39. Mujahid, K., Rasheed, M. S., Sabir, A., Nam, J., Ramzan, T., Ashraf, W., & Imran, I. (2025). Cannabidiol as an immune modulator: A comprehensive review. *Saudi Pharm J*, *33*(3), 11. https://doi.org/10.1007/s44446-025-00005-7
40. Yu, M., Zhang, Y., Fang, M., Jehan, S., & Zhou, W. (2022). Current Advances of Nanomedicines Delivering Arsenic Trioxide for Enhanced Tumor Therapy. *Pharmaceutics*, *14*(4), 743. https://doi.org/10.3390/pharmaceutics14040743
41. Han, M., Zhang, Z., Li, X., Tong, H., Xu, Z., Ding, Z., & Wang, X. (2022). Effects of collagen peptides from Micropterus salmoides skin on oxidative damage induced by cyclophosphamide in mice. *Front Nutr*, *9*, 1037212. https://doi.org/10.1016/S0168-3659(99)00248-5
42. Jiang, T., Zhou, C., & Ren, S. (2016). Role of IL-2 in cancer immunotherapy. *Oncoimmunology*, *5*(6), e1163462. https://doi.org/10.1080/2162402X.2016.1163462

Figures

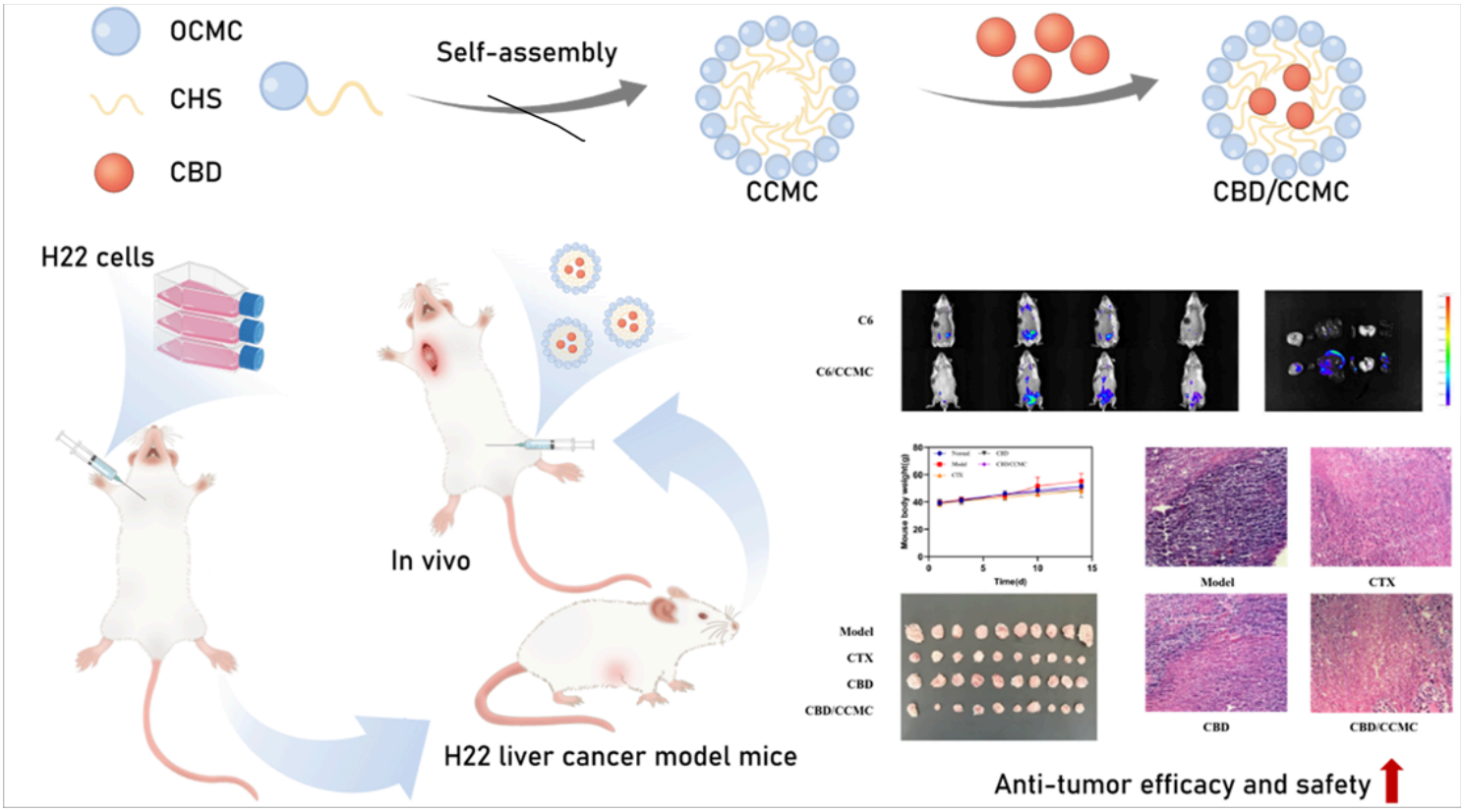


Figure 1

Graphical abstract.

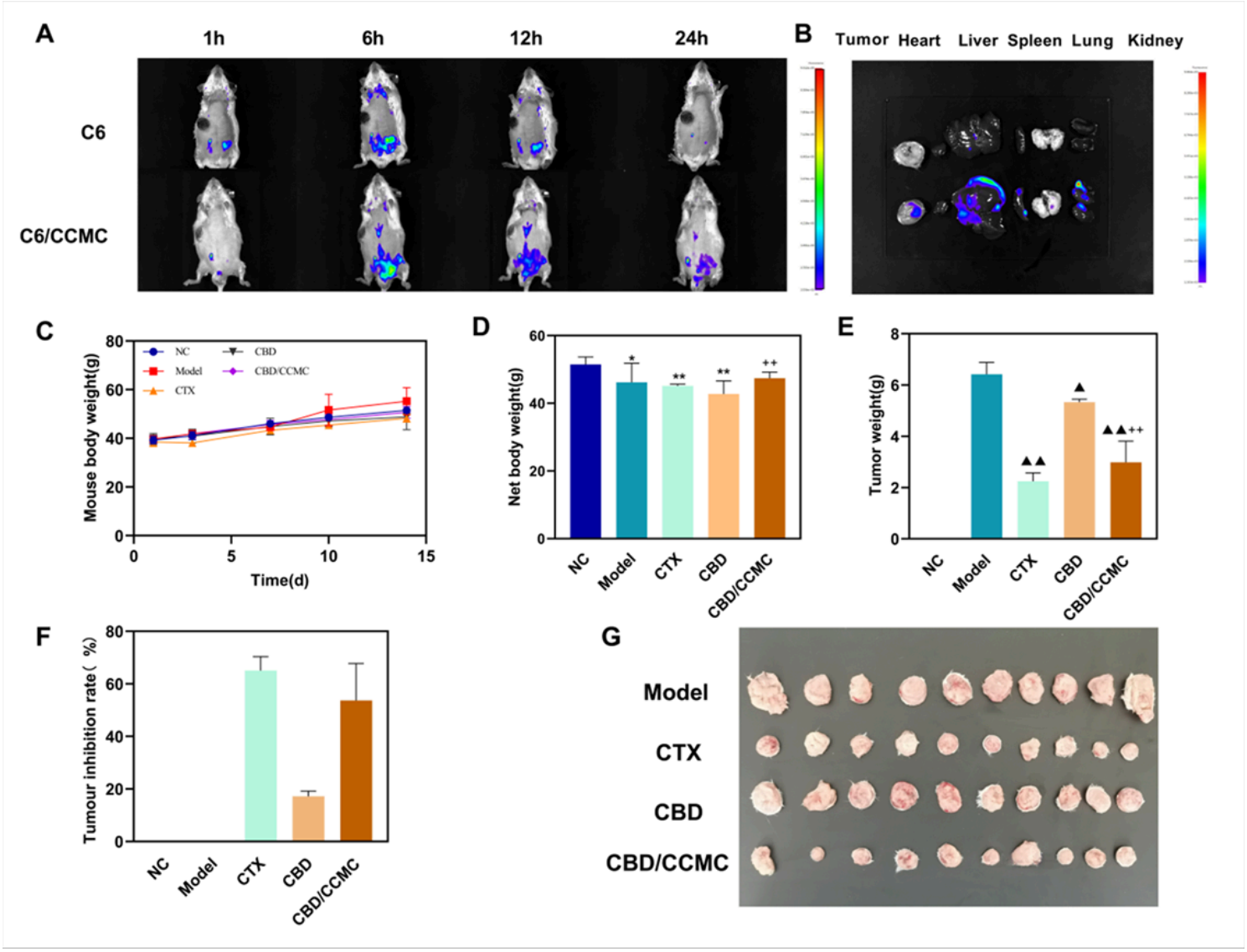


Figure 2

In vivo biodistribution and anti-tumor efficacy of CBD/CCMC nanomicelles. (A) Whole-body fluorescence imaging; (B) Ex vivo organ imaging; (C) Mouse body weight changes; (D) Net body weight; (E) Tumor weight; (F) Tumor inhibition rate; (G)Representative photographs of tumors. Compared with the NC group, $^{*}P<0.05$, $^{**}P<0.01$; Compared with the Model group, $▲P<0.05$, $▲▲P<0.01$; Compared with the CBD group, $^{+}P<0.05$, $^{++}P<0.01$.

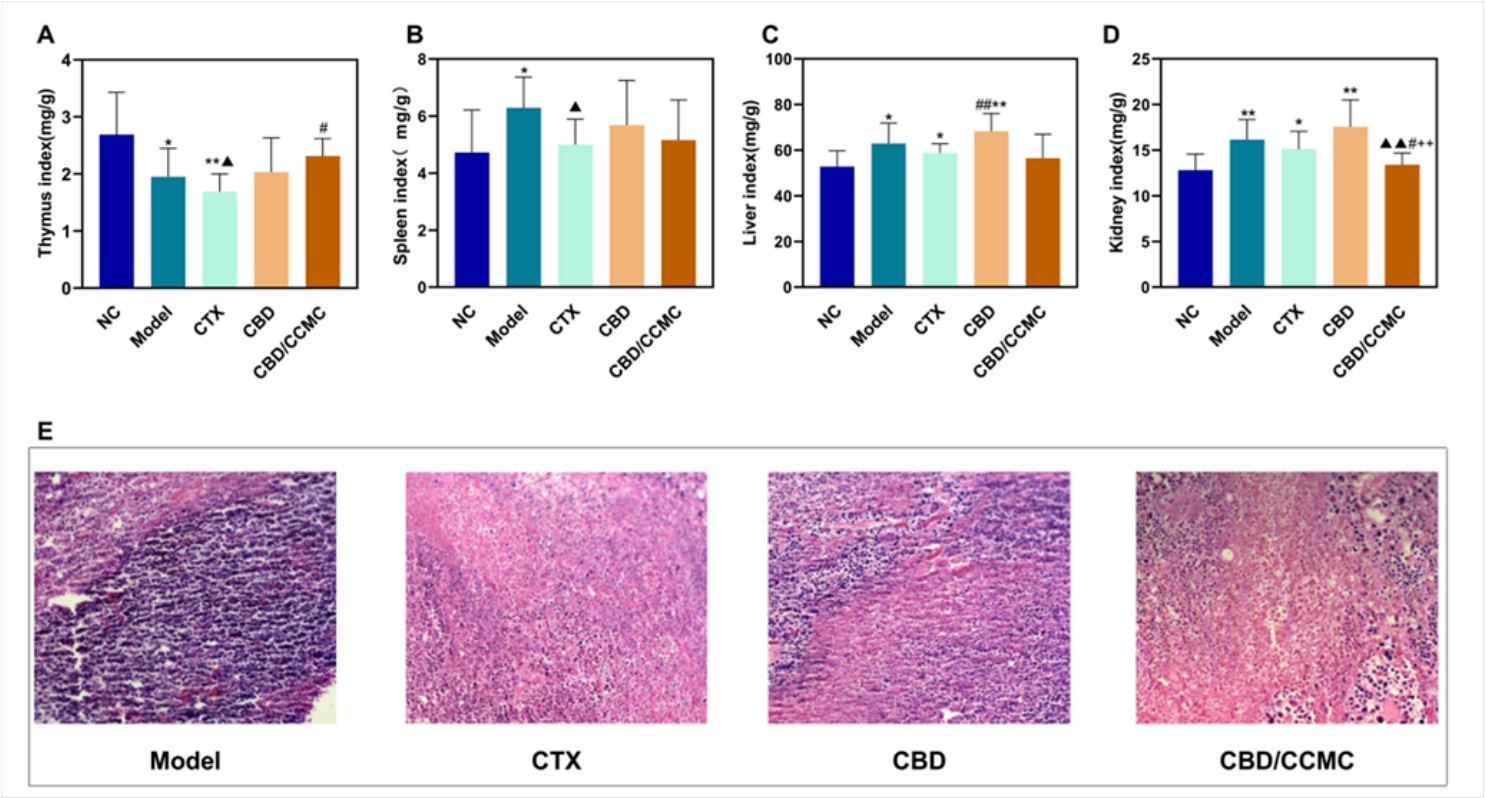


Figure 3

Organ index: (A) Thymus index, (B) Spleen index, (C) Liver index, (D) Kidney index. (E) HE staining images of tumor tissue after treatment (scale bar: 200 μm). Compared with the NC group, $^{*}P<0.05$, $^{**}P<0.01$; Compared with the Model group, $^{▲}P<0.05$, $^{▲▲}P<0.01$; Compared with the CTX group, $^{\#}P<0.05$, $^{\#\#}P<0.01$; Compared with the CBD group, $^{+}P<0.05$, $^{++}P<0.01$.

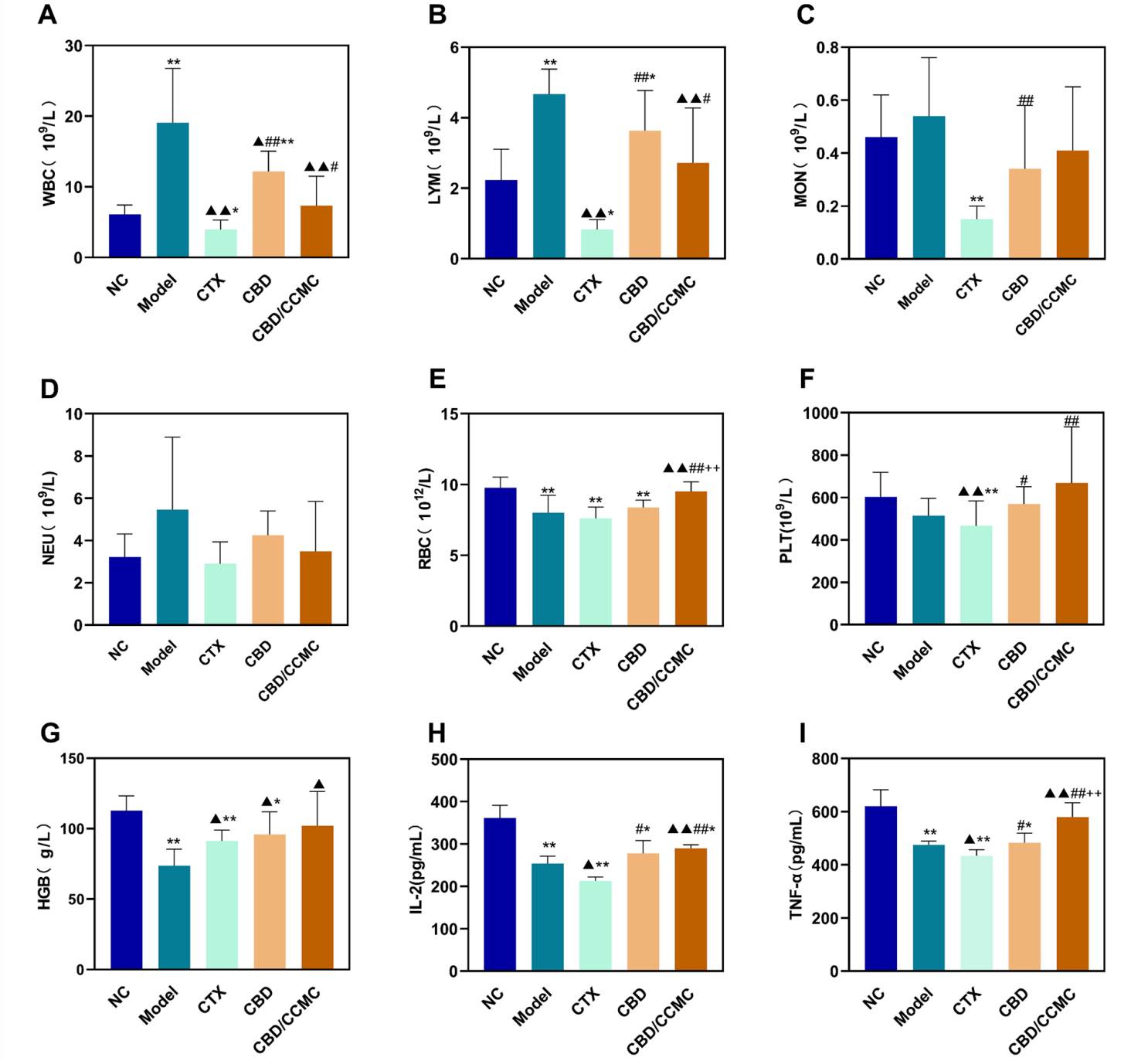


Figure 4

Blood analysis results *in vivo*: (A) WBC, white blood cells; (B) LYM, lymphocytes; (C) MON, monocytes; (D) NEU, Neutrophil; (E) RBC, red blood cells; (F) PLT, platelets; (G) HGB, hemoglobin; Effect of nanomicelles on the levels of serum cytokines: (H) IL-2, (I) TNF-α. Compared with the NC group, $^{*}P<0.05$, $^{**}P<0.01$; Compared with the Model group, $^{▲}P<0.05$, $^{▲▲}P<0.01$; Compared with the CTX group, $^{\#}P<0.05$, $^{\#\#}P<0.01$; Compared with the CBD group, $^{+}P<0.05$, $^{++}$ <0.01.